J|A|C|S
ARTICLES
Published on Web 01/17/2002

Metallacycles of Porphyrins as Building Blocks in the Construction of Higher Order Assemblies through Axial Coordination of Bridging Ligands: Solution- and Solid-State Characterization of Molecular Sandwiches and Molecular Wires

Elisabetta Iengo, Ennio Zangrando, Romina Minatel, and Enzo Alessio*

Contribution from the Dipartimento di Scienze Chimiche, Università di Trieste, Via L. Giorgieri 1, 34127 Trieste, Italy

Received May 9, 2001

Abstract: Treatment of the octahedral Ru(II)−dimethyl sulfoxide complexes *trans*-$RuCl_2$(dmso-S)$_4$ (**1**), *trans*-$RuCl_2$(dmso-O)$_2$(CO)$_2$ (**2**), and *trans*-$RuCl_2$(dmso)$_3$(CO) (**3**) with a stoichiometric amount of 5,10-bis(4′-pyridyl)-15,20-diphenylporphyrin (4′-*cis*-DPyP) yields, after chromatographic purification, the novel 2+2 molecular squares of formula [*trans,cis,cis*-$RuCl_2$(dmso-S)$_2$(4′-*cis*-DPyP)]$_2$ (**4**), [*trans,cis,cis*-$RuCl_2$(CO)$_2$-(4′-*cis*-DPyP)]$_2$ (**5**), and [*trans,cis,cis*-$RuCl_2$(dmso-S)(CO)(4′-*cis*-DPyP)]$_2$ (**6**), respectively. Compound **6** exists as an equimolar mixture of the isomeric metallacycles **6a** and **6b**, depending on whether the 4′-N(py) rings of 4′-*cis*-DPyP's are trans to CO or to dmso-S. Compounds **4**−**6** were fully characterized by NMR and IR spectroscopy and by FAB mass spectrometry. Treatment of **5** with excess zinc acetate in chloroform/methanol mixtures led to the isolation of the corresponding zinc adduct [*trans,cis,cis*-$RuCl_2$(CO)$_2$(Zn·4′-*cis*-DPyP)]$_2$ (**5Zn**). Treatment of **5Zn** with 1 equiv of a trans ditopic N-donor ligand **L** (**L** = 4,4′-bipy, 5,15-bis(4′-pyridyl)-2,8,12,18-tetra-*n*-propyl-3,7,13,17-tetramethylporphyrin (4′-*trans*-DPyP-npm), or 5,15-bis(4′-pyridyl)-10,20-diphenylporphyrin (4′-*trans*-DPyP)) leads readily and selectively, according to ^{1}H NMR spectroscopy, to the quantitative assemblying of 2:2 supramolecular adducts of stacked metallacycles of formula [(**5Zn**)$_2$(μ-**L**)$_2$] (**7**−**9**), which were thoroughly characterized in solution by NMR spectroscopy. NMR features indicate that, at ambient temperature, the equilibrium between **5Zn** and **L** to yield [(**5Zn**)$_2$(μ-**L**)$_2$] has an intermediate to slow rate on the NMR time scale (relatively broad signals for **L**) and is totally shifted toward the 2:2 product (all or nothing process). Single-crystal X-ray investigations showed that, depending on the nature of the bridging ligand, in the solid state these sandwich structures can either be maintained or originate polymeric chains formulated as [(**5Zn**)(μ-**L**)]$_\infty$. When **L** = 4′-*trans*-DPyP, both solution- and solid-state data indicate that [(**5Zn**)$_2$(μ-4′-*trans*-DPyP)$_2$] (**9**) is a discrete supramolecular assembly of two molecular squares of metalloporphyrins axially connected through other porphyrins. In this molecular box, the two bridging porphyrins are coplanar at a distance of about 11.4 Å. When **L** = 4,4′-bipy, the corresponding adduct **7** has the anticipated sandwich-like discrete architecture [(**5Zn**)$_2$(μ-4,4′-bipy)$_2$] in solution, but it assumes a stairlike polymeric wire structure in the solid state. The polymer [(**5Zn**)(μ-4,4′-bipy)]$_\infty$ is made by **5Zn** squares bridged by 4,4′-bipy ligands which are axially coordinated alternatively on the two opposite sides of each square. Our work clearly established that relatively simple supramolecular adducts of porphyrins, such as molecular squares, are suitable building blocks for the construction of more elaborate assemblies of higher order by axial coordination of bridging ligands.

Introduction

Central to supramolecular chemistry[1,2] is the concept that assemblies of molecular components (supramolecular structures) can be designed to perform relatively elaborate and useful tasks. The concept is currently being applied to the design of supramolecular systems (molecular devices) capable of mimicking, at the molecular level, functions normally performed by natural systems or by artificial macroscopic devices (e.g., molecular-level machines).[3] Thus, supramolecular chemistry can be viewed as the basis for a "bottom-up" approach to the challenging fields of molecular electronics[4] and nanotechnology. Moreover, the formation of supramolecular entities represents an abiological analogue of numerous biological processes mediated by collective interactions and recognition events between large molecules. From a synthetic standpoint, recent

* To whom correspondence should be addressed. Phone: +39 040 6763961. Fax: +39 040 6763903. Email: alessi@univ.trieste.it.

(1) Lehn, J.-M. *Supramolecular Chemistry, concepts and perspectives*; VCH: Weinheim, Germany, 1995.
(2) *Comprehensive Supramolecular Chemistry*; Atwood, J. L., Davies, J. E. D., MacNicol, D. D., Vögtle, F., Eds.; Pergamon/Elsevier: Oxford, 1996.
(3) Balzani, V.; Credi, A.; Raymo, F. M.; Stoddart, J. F. *Angew. Chem., Int. Ed.* **2000**, *39*, 3348−3391.
(4) Tour, J. M. *Acc. Chem. Res.* **2000**, *33*, 791−804.

years have witnessed a growing number of supramolecular systems that incorporate metal ions as assembling and organizing centers.[5]

Supramolecular systems containing porphyrins and metalloporphyrins are particularly attractive because the components can introduce photochemical and redox properties. In fact, porphyrins offer a variety of desirable features such as a rigid, planar geometry, high stability, an intense electronic absorption, a strong fluorescence emission, and a small HOMO−LUMO energy gap, as well as flexible tunability of their optical and redox properties by appropriate metalation. Synthetic multiporphyrin assemblies are investigated in materials science and nanotechnology (e.g., molecular-scale electronics, optical devices, sensors), where the establishment of pathways for the controlled access to nanosized chemical entities is of paramount interest;[6] in particular, light-induced functions have attracted a great deal of interest.[7] Further potential applications exist, for example, as models of naturally occurring multichromophore aggregates, such as the photosynthetic reaction center (photoinduced electron transfer)[8] and the light harvesting complex of purple bacteria.[9] In particular, there has been substantial recent interest in the construction of cyclic multiporphyrin assemblies which have the chromophores locked in a mutually coplanar geometry,[10] since a wheel-shaped oligomeric porphyrinoid architecture is found in light-harvesting proteins.[11]

The metal-mediated self-assembly, which exploits the formation of coordination bonds between peripheral basic site(s) on the porphyrins and metal centers, is an attractive highly convergent synthetic approach that has lately provided many new examples of large assemblies of porphyrins.[12−15] The final shape and dimension of the self-assembled architecture is defined by the metal coordination geometry (the metal center may belong either to a metalloporphyrin or to a coordination complex) and by the number and relative orientations of the peripheral sites on the porphyrins. Solution studies on discrete assemblies obtained by this approach have focused mainly on electron and energy transfer and on host−guest interactions.[12] On the other hand, design strategies to develop solid-state multichromophoric arrays of defined rigidity, dimensionality, porosity, and selectivity are also actively investigated.[13−15]

Within this framework, meso-pyridyl/phenyl porphyrins (PyP's) proved to be particularly versatile building blocks.[16] In particular, the self-assembly of 4′-bispyridylporphyrins, i.e., porphyrins bearing two peripheral basic sites either at 90° (5,10-bis(4′-pyridyl)-15,20-diphenylporphyrin = 4′-*cis*-DPyP) or at 180° (5,15-bis(4′-pyridyl)-10,20-diphenylporphyrin = 4′-*trans*-DPyP) from one another, with coordination compounds having two readily available coordination sites in cis or trans geometry has led to the formation of a series of 2+2 and 4+4 molecular squares, in which the porphyrins occupy either the sides[17−19] or the corners[17,20,21] of the metallacycle.

In previous papers we described discrete supramolecular architectures obtained by coordination of PyP's to metalloporphyrins (side-to-face assemblies)[22−26] and/or to coordination compounds.[26−29]

We report now on the synthesis and characterization of 2+2 homometallic molecular squares of porphyrins obtained by self-assembly of 4′-*cis*-DPyP with neutral Ru(II) octahedral complexes. We also show how these discrete units, after metalation of the porphyrins, are suitable building blocks for the construction of more elaborate assemblies of higher order by axial coordination of bridging ligands.

Results and Discussion

We recently reported that treatment of the octahedral Ru(II)−dimethyl sulfoxide complexes *trans*-$RuCl_2$(dmso-S)$_4$ (**1**), *trans*-$RuCl_2$(dmso-O)$_2$(CO)$_2$ (**2**), and *trans*-$RuCl_2$(dmso)$_3$(CO) (**3**) with an excess of 4′-*cis*-DPyP yields the bisporphyrin adducts *trans,cis,cis*-$RuCl_2$(X)(Y)(4′-*cis*-DPyP)$_2$ (X = Y = dmso-S, **1a**; X = Y = CO, **2a**; and X = dmso-S, Y = CO, **3a**; *trans,cis*-$RuCl_2$(X)(Y) = ***t*Ru**). These compounds were further reacted with the square planar complex of Pd(II), Pd(dppp)(OTf)$_2$ (dppp = 1,3-bis(diphenylphosphanyl)propane, OTf = trifluoromethanesulfonate = triflate), to give the corresponding 2+2 heterobimetallic cationic molecular squares of formula [***t*Ru**(4′-*cis*-DPyP)$_2$Pd(dppp)](OTf)$_2$ (Scheme 1).[28] The reaction between equimolar amounts of **1**−**3** and 4′-*cis*-DPyP is now investigated.

Design and Synthesis of Porphyrin Metallacycles. Treatment of 4′-*cis*-DPyP with a stoichiometric amount of **1**−**3** led to the formation of the corresponding 2+2 homonuclear neutral

(5) For recent review articles, see: (a) Leininger, S.; Olenyuk, B.; Stang, P. J. *Chem. Rev.* **2000**, *100*, 853−908. (b) Swiegers G. F.; Malefetse, T. J. *Chem. Rev.* **2000**, *100*, 3483−3537. (c) Fujita, M. *Chem. Soc. Rev.* **1998**, *27*, 417−425. (d) Stang, P. J. *Chem. Eur. J.* **1998**, *4*, 19−27.
(6) (a) Chou, J.-H.; Kosal, M. E.; Nalwa, H. S.; Rakow, N. A.; Suslick, K. S. In *The Porphyrin Handbook*; Kadish, K. M., Smith, K. M., Guillard, R., Eds.; Academic Press: New York, 1999; Vol. 6, p 42. (b) Vicente, M. G. H.; Jaquinod, L.; Smith, K. M. *Chem Commun.* **1999**, 1771−1782.
(7) Balzani, V.; Scandola, F. *Supramolecular Photochemistry*; Horwood: Chichester, U.K., 1991.
(8) (a) Wasielewski, M. R. *Chem. Rev.* **1992**, *92*, 435−461. (b) Harriman, A.; Sauvage, J. P. *Chem. Soc. Rev.* **1996**, 41−48.
(9) (a) Seth, J.; Palaniappan, V.; Johnson, T. E.; Prathapan, S.; Lindsey, J. S.; Bocian, D. F. *J. Am. Chem. Soc.* **1994**, *116*, 10578−10592. (b) Hsiao, J.-S.; Krueger, B. P.; Wagner, R. W.; Johnson, T. E.; Delaney, J. K.; Mauzerall, D. C.; Fleming, G. R.; Lindsey, J. S.; Bocian, D. F.; Donohoe, R. J. *J. Am. Chem. Soc.* **1996**, *118*, 11181−11193. (c) Nakano, A.; Osuka, A.; Yamazaki, I.; Yamazaki, T.; Nishimura, Y. *Angew. Chem., Int. Ed.* **1998**, *37*, 3023−3027. (d) Kuciauskas, D.; Liddell, P. A.; Lin, S.; Johnson, T. E.; Weghorn, S. J.; Lindsey, J. S.; Moore, A.; Moore, T. A.; Gust, D. *J. Am. Chem. Soc.* **1999**, *121*, 8604−8614.
(10) (a) Wagner, R. W.; Seth, J.; Yang, S. I.; Kim, D.; Bocian, D. F.; Holten, D.; Lindsey J. S. *J. Org. Chem.* **1998**, *63*, 5042−5049. (b) Sugiura, K.; Fujimoto, Y.; Sakata Y. *Chem. Commun.* **2000**, 1105−1106.
(11) Pullerits, T.; Sundström V. *Acc. Chem. Res.* **1996**, *29*, 381−389.
(12) For a comprehensive recent review, see: Chambron, J.-C.; Heitz, V.; Sauvage J.-P. In *The Porphyrin Handbook*; Kadish, K. M., Smith, K. M., Guillard, R., Eds.; Academic Press: New York, 2000; Vol. 6, Chapter 40.
(13) Sharma, C. V. K.; Broker, G. A.; Huddleston, J. G.; Baldwin, J. W.; Metzger, R. M.; Rogers R. D. *J. Am. Chem. Soc.* **1999**, *121*, 1137−1144.
(14) Pan, L.; Nool, B. C.; Wang X. *Chem. Commun.* **1999**, 157−158.
(15) Krishna Kumar, R.; Goldberg I. *Angew. Chem., Int. Ed.* **1998**, *37*, 3027−3030.
(16) Fleischer, E. B.; Shacter, A. M. *Inorg. Chem.* **1991**, *30*, 3763−3769.
(17) Drain, C. M.; Lehn, J.-M. *J. Chem. Soc., Chem. Commun.* **1994**, 2313−2315.
(18) Slone, R. V.; Hupp, J. T. *Inorg. Chem.* **1997**, *36*, 5422−5423.
(19) Stang, P. J.; Fan, J.; Olenyuk, B. *Chem. Commun.* **1997**, 1453−1454.
(20) Schmitz, M.; Leininger, S.; Fan, J.; Arif, A. M.; Stang, P. J. *Organometallics* **1999**, *18*, 4817−4824.
(21) Fan, J.; Whiteford, J. A.; Olenyuk, B.; Levin, M. D.; Stang, P. J.; Fleisher, E. B. *J. Am. Chem. Soc.* **1999**, *121*, 2741−2752.
(22) Alessio, E.; Macchi, M.; Heath, S.; Marzilli, L. G. *Chem. Commun.* **1996**, 1411−1412.
(23) Alessio, E.; Geremia, S.; Mestroni, S.; Iengo, E.; Srnova, I.; Slouf, M. *Inorg. Chem.* **1999**, *38*, 869−875.
(24) Alessio, E.; Geremia, S.; Mestroni, S.; Srnova, I.; Slouf, M.; Gianferrara, T.; Prodi, A. *Inorg. Chem.* **1999**, *38*, 2527−2529.
(25) Prodi, A.; Indelli, M. T.; Kleverlaan, C. J.; Scandola, F.; Alessio, E.; Gianferrara, T.; Marzilli, L. G. *Chem. Eur. J.* **1999**, *5*, 2668−2679.
(26) Alessio, E.; Ciani, E.; Iengo, E.; Kukushkin, V. Yu.; Marzilli. L. G. *Inorg. Chem.* **2000**, *39*, 1434−1443.
(27) Alessio, E.; Macchi, M.; Heat, S. L.; Marzilli, L. G. *Inorg. Chem.* **1997**, *36*, 5614−5623.
(28) Iengo, E.; Milani, B.; Zangrando, E.; Geremia, S.; Alessio, E. *Angew. Chem., Int. Ed.* **2000**, *39*, 1096−1099.
(29) Iengo, E.; Minatel, R.; Milani, B.; Marzilli, L. G.; Alessio E. *Eur. J. Inorg. Chem.* **2001**, 609−612.

Scheme 1. Reaction Pathways of 4′-*cis*-DPyP with Ru(II) Compounds **1**−**3** Leading Either to 2+2 Molecular Squares **4**−**6** (Left) or to the Bisporphyrin Adducts **1a**−**3a** (Right)[a]

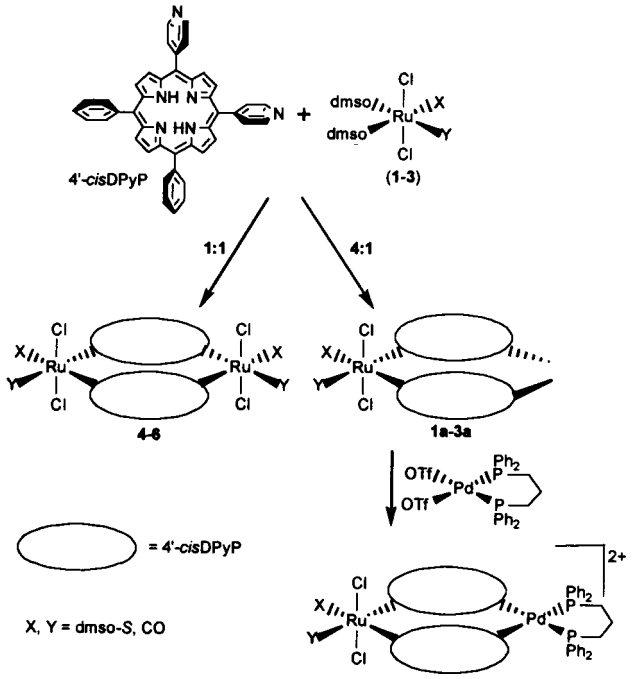

[a] Treatment of **1a**−**3a** with an appropriate square planar Pd(II) complex yields the corresponding 2+2 heterobimetallic molecular squares.

squares of porphyrins of formula [*trans,cis,cis*-$RuCl_2$(X)(Y)-(4′-*cis*-DPyP)]$_2$ (X = Y = dmso-S, **4**; X = Y = CO, **5**; and X = dmso-S, Y = CO, **6**) (Scheme 1). These products were purified by column chromatography and fully characterized by means of NMR spectroscopy and FAB mass spectrometry. The case of [*trans,cis,cis*-$RuCl_2$(dmso-S)$_2$(4′-*cis*-DPyP)]$_2$ (**4**) will be discussed in more detail.

The reaction between 4′-*cis*-DPyP and *trans*-$RuCl_2$(dmso-S)$_4$ (**1**) was monitored by TLC analysis. Consumption of 4′-*cis*-DPyP (R_f = 0.22) was accompanied by the build-up of a main product, characterized by a relatively large R_f (0.72); some minor products, with similar and much lower R_f's, were also found. In general, the mobility of pyridylporphyrin adducts on silica gel is inversely related to the number of free 4′-N(py) sites. Thus, the most abundant and mobile product of the above reaction was attributed to a metallacyclic species and the minor spots to open-chain species with unbound 4′-N(py) sites. The ^{1}H NMR spectrum of the crude reaction product showed sharp resonances, attributed to the molecular square **4**, together with broad signals associated to the presence of oligomeric side products. Compound **4** was easily obtained in pure form by column chromatography. The ^{1}H NMR spectrum of **4** unambiguously established its metallacyclic nature and high symmetry (D_{2h}) (Figure 1): (i) no signals for unbound pyridyl rings are present; the H2,6 and the H3,5 resonances of the 4′-N(py) rings are downfield shifted, as expected for coordination to the ***t*Ru** moieties ($\Delta\delta$ = 1.01 and 0.25, respectively) compared to unbound 4′-*cis*-DPyP;[27] (ii) only one set of signals for the porphyrin protons[30] and one singlet for S-bonded dmso (δ = 3.65) are observed, indicating the equivalence of the chromophores and the sulfoxide molecules; (iii) according to integration, there are two dmso-S molecules for each porphyrin unit; (iv) the resonances of the pyrrole protons (βH), two singlets and two doublets of equal intensity (partially overlapped), are consistent with a cis geometry for each porphyrin ring. A FAB mass spectrum confirmed the 2+2 nuclearity of the adduct (*m*/*z* = 1892.1, calculated 1890).

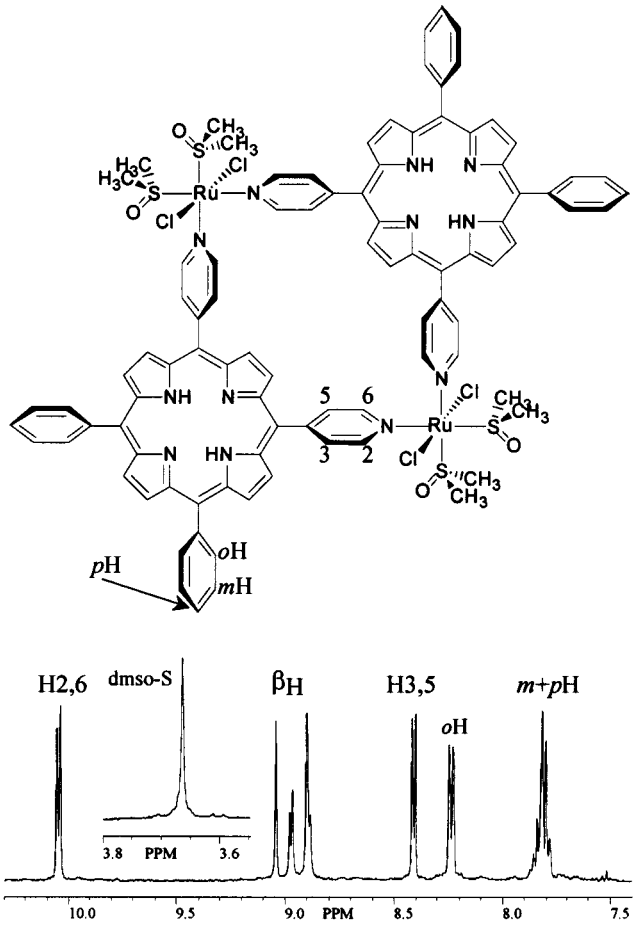

Figure 1. Schematic drawing of [*trans,cis,cis*-$RuCl_2$(dmso-S)$_2$(4′-*cis*-DPyP)]$_2$ (**4**) with labeling scheme and its ^{1}H NMR spectrum (with the exception of the NH resonance) in $CDCl_3$ (ppm).

The ^{1}H NMR spectrum of the crude reaction mixture between *trans,cis,cis*-$RuCl_2$(dmso-O)$_2$(CO)$_2$ (**2**) and an equimolar amount of 4′-*cis*-DPyP clearly indicated the presence of three major products with sharp and resolved resonances pertaining to cyclic symmetrical species, besides smaller amounts of open-chain oligomers with broad signals. Correspondingly, in the TLC analysis, three spots with large and similar R_f's were detected. The product with the largest R_f (0.72), which is also the most abundant, was separated and purified by column chromatography and characterized as the molecular square [*trans,cis,cis*-$RuCl_2$(CO)$_2$(4′-*cis*-DPyP)]$_2$ (**5**). Apart from the absence of the dmso signal, the ^{1}H NMR spectrum of **5** is substantially similar to that of **4** and consistent with a metallacyclic geometry of D_{2h} symmetry. The high symmetry of **5** is apparent also from its ^{13}C{^{1}H} NMR spectrum, in which a single carbon resonance for the equivalent CO groups is observed at δ = 194.5. In the IR spectrum in chloroform solution, two carbonyl stretching bands are detected at 2073 and 2013 cm^{-1}, as expected for a cis geometry of the two CO molecules on each ***t*Ru** unit. The FAB MS of **5** confirmed the nuclearity of the adduct (*m*/*z* =

(30) Contrary to what was found in **1a**−**3a** (see ref 28), the *o*H and the *m*+*p*H phenyl resonances of **4**−**6** are not split into two multiplets each, confirming that the chromophores are not free to rotate about the Ru−N bonds (see ref 27).

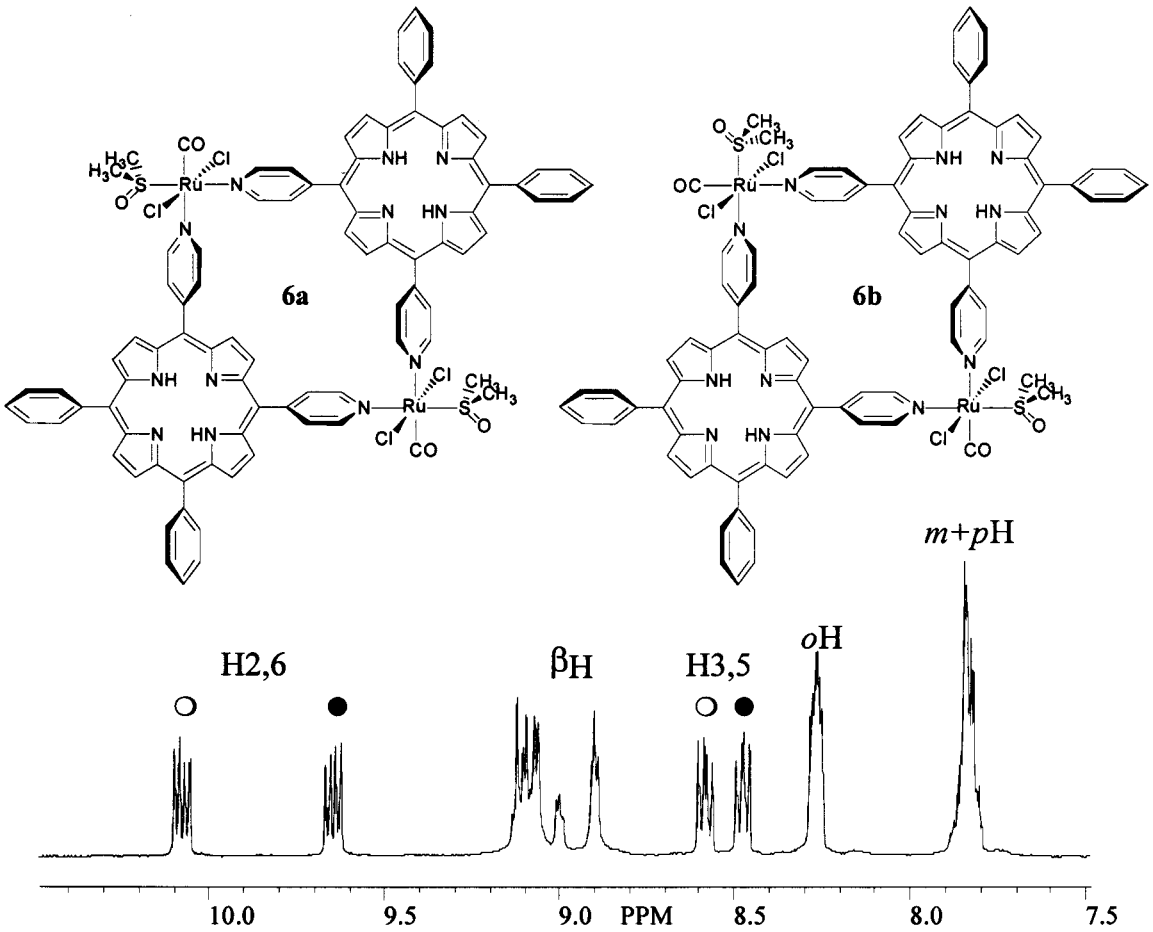

Figure 2. Schematic drawing of the two geometrical isomers of [*trans*,*cis*,*cis*-$RuCl_2$(dmso-S)(CO)(4′-*cis*-DPyP)]$_2$ (**6**), **6a** and **6b**, and ^{1}H NMR spectrum of their equimolar mixture. See Figure 1 for labeling scheme; ○ = trans to dmso-S, ● = trans to CO.

1691.2, calculated 1690). Purification and characterization of the other metallacyclic products are in progress and will be discussed elsewhere.

Finally, treatment of *trans*,*cis*,*cis*-$RuCl_2(dmso)_3(CO)$ (**3**) with equimolar amounts of 4′-*cis*-DPyP led, after column purification, to the isolation of [*trans*,*cis*,*cis*-$RuCl_2$(dmso-S)(CO)(4′-*cis*-DPyP)]$_2$ (**6**) as an equimolar mixture of the isomeric molecular squares **6a** and **6b** (Figure 2). Indeed, when the X and Y ligands on the ***t*Ru** unit are different from one another, two geometrical isomers are possible: in one case (**6a**), the 4′-N(py) moieties of each porphyrin are trans to one CO and one dmso-S ligand, respectively, and the resulting metallacycle has a C_{2v} symmetry; in the other case (**6b**), the two 4′-N(py) ligands of one 4′-*cis*-DPyP are trans to CO, while those of the other are trans to dmso-S, and the resulting molecular square has a C_{2h} symmetry. The two isomers could not be separated by column chromatography. In the aromatic region of the NMR spectrum of the mixture of **6a** and **6b**, four equally intense multiplets attributed to pyridyl protons are found (Figure 2).[31] By comparison with the spectra of **4** and **5**, the multiplets at $\delta = 10.08$ and $\delta = 8.58$, correlated in the H−H COSY spectrum, were assigned to the H2,6 and H3,5, respectively, of the pyridyl rings trans to dmso-S; similarly, the multiplets at $\delta = 9.65$ and $\delta = 8.47$ were assigned to the H2,6 and H3,5, respectively, of the pyridyl rings trans to CO. Indeed, each of these resonances consists of two close multiplets of equal intensity, one belonging to **6a** and the other belonging to **6b** (Figure 2); assignment of these resonances to the two isomers was not possible. All the other ^{1}H NMR resonances of **6a** and **6b** overlap. Also the $^{13}C\{^1H\}$ NMR signals of **6a** and **6b** for the CO groups ($\delta = 200.6$) and the dmso methyl groups ($\delta = 47.5$) overlap. In the IR spectrum in chloroform solution, one broad band relative to C═O stretching was detected at 1990 cm^{-1}. The FAB mass spectrum confirmed the nuclearity of **6** ($m/z = 1790.5$, calculated 1790).

The electronic absorption spectra of **4**−**6** are very similar to that of 4′-*cis*-DPyP, apart from a small bathochromic shift for the Soret band (ca. 8 nm); the molar extinction coefficient per porphyrin in each square (ϵ/por for the Soret band) is substantially the same as that found for 4′-*cis*-DPyP ($\epsilon = 29 \times 10^4$ cm^{-1} M^{-1}). A detailed investigation of the photophysical properties of molecular squares **4** and **5** is being reported elsewhere.[32]

Treatment of **5** with excess zinc acetate in chloroform/methanol mixtures led to the isolation of the corresponding zinc adduct, [*trans*,*cis*,*cis*-$RuCl_2(CO)_2$(Zn·4′-*cis*-DPyP)]$_2$ (**5Zn**). The same reaction was not pursued on **4** and **6** since, as previously reported by us for other Zn·PyP−Ru−dmso-S complexes, a self-assembling process is expected to occur between the oxygen atom of the dmso-S ligand of one molecule and the zinc center of another molecule.[27] Such a relatively weak interaction induces, nevertheless, a broadening of some NMR resonances,

(31) Despite the different symmetry of **6a** and **6b**, the same NMR pattern is expected for the pyridyl protons of the two metallacycles.

(32) Prodi, A.; Kleverlaan, C. J.; Indelli, M. T.; Scandola, F.; Alessio, E.; Iengo, E. *Inorg. Chem.* **2001**, *40*, 3498−3504.

thus resulting in a more complicated general spectral pattern. The ^{1}H NMR spectrum of **5Zn** is very similar to that of **5** except for a slight downfield shift of the pyrrole proton resonances and, of course, for the absence of the −NH signal. The resonances of **5Zn** are always sharp, and the spectrum is concentration independent in the range 0.1−10 mM (as was the case for **4**-**6**), indicating that no aggregation occurs in chloroform solution.

Self-Assembling of Molecular Squares by Axial Ligation. In general, the insertion of metal ions into the porphyrin cores, in addition to changing the redox and photophysical parameters of the metallacycle, introduces new acceptor centers for further reactions. The number of coordination axial sites (one or two) that can be exploited, and their lability as well as the affinity toward different donor atoms, can be fine-tuned by changing the nature and the oxidation state of the metal centers inserted into the porphyrin cores.[33] In particular, zinc porphyrins prefer nitrogen donor ligands, adopt five-coordinate square pyramidal geometry, and are kinetically relatively labile. Thus, **5Zn** is a building block with two acceptor sites that can be treated with appropriate multidentate donor ligands for the construction of more elaborate supramolecular adducts.

Although oligomers[16,34] and polymers (molecular wires)[35] of metalloporphyrins axially connected through bridging ligands have been described, there are few examples concerning multiporphyrin systems. Anderson and Sanders described the induced-fit binding of bis-amine ligands inside a series of flexible polymacrocyclic zinc porphyrin hosts; coordination of the bridging ligand induced conformational changes leading to a cofacial disposition of the metalloporphyrins involved.[36] With the aim of increasing the interporphyrin conjugation, Anderson and co-workers also extensively investigated the assembly of two flexible oligomers of covalently connected zinc porphyrins through axial ligation of bridging N-donor ligands, thus obtaining 2D molecular ladder systems.[37] To date, however, the stacking of 2D porphyrin macrocycles through axial ligation to yield 3D assemblies has been scarcely investigated; examples concerning the use of molecular squares of metalloporphyrins[17] and closely related systems, such as molecular grids,[38] have been alluded to only briefly and are not well documented.

The reactivity of **5Zn** toward a series of ditopic N-donor ligands (**L**) with a trans geometry, namely 4,4′-bipy, 4′-*trans*-DPyP-npm (5,15-bis(4′-pyridyl)-2,8,12,18-tetra-*n*-propyl-3,7,-13,17-tetramethylporphyrin), and 4′-*trans*-DPyP, was monitored by ^{1}H NMR spectroscopy. Addition of less than stoichiometric amounts of **L** to a $CDCl_3$ solution of **5Zn** induces the appearance of some relatively broad signals, which sharpen upon lowering the temperature. Below −20 °C, two sets of resonances are detected, one relative to **5Zn** and the other assigned to the 2:2 supramolecular adduct of general formula $[(\mathbf{5Zn})_2(\mu\text{-}\mathbf{L})_2]$ (**7**−**9**), consisting of two molecular squares connected face-to-face by two bridging ligands which are axially bound to the metalloporphyrins (Scheme 2). No signals relative to uncoordinated **L** or to reaction intermediates are observed.

Scheme 2 [a]

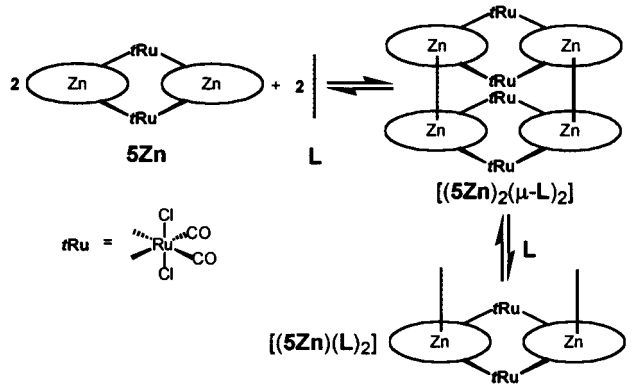

[a] Porphyrins are represented with ovals; ***t*Ru** = *trans,cis,cis*-$RuCl_2(CO)_2$.

When the stoichiometric ratio between **5Zn** and **L** is reached, only one set of resonances is observed, corresponding to the complete formation of $[(\mathbf{5Zn})_2(\mu\text{-}\mathbf{L})_2]$. These resonances are still relatively broad at room temperature but become sharp and well-resolved on lowering the temperature below −20 °C. Complete assignment was made possible by 2D H−H COSY and EXSY experiments. The case of $[(\mathbf{5Zn})_2(\mu\text{-}4,4'\text{-bipy})_2]$ (**7**) will be discussed in greater detail.

The main features of the NMR spectrum of **7** (Figure 3), which unambiguously establish the geometry of the adduct, are the following: (i) relative integration of 4,4′-bipy and of porphyrin signals indicates that there is one molecule of bridging ligand every two porphyrin units; (ii) the two bridging 4,4′-bipy ligands give rise to two equally intense resonances only, implying that they are equivalent to each other and symmetrically coordinated; (iii) axial coordination of bipy is unequivocally indicated by the large upfield shift of H2,6 and H3,5 resonances ($\Delta\delta = -6.76$ and -2.35, respectively; $T = -40$ °C) due to the combined ring currents of both porphyrins; (iv) all porphyrins are equivalent and give only one set of signals which are slightly upfield shifted as compared to those of **5Zn**. This is consistent with a cofacial disposition of the two molecular squares which induces a mutual shielding of the porphyrin cores.[37]

Each resonance of the meso aromatic rings of 4′-*cis*-DPyP in **7**, relatively broad at room temperature, splits into two sharp signals of equal intensity on lowering the temperature below −20 °C (Figure 3). These splittings can be well explained by considering the sandwich structure proposed for **7**. In fact, since the meso pyridyl and phenyl rings like to stay normal to the porphyrin plane due to steric interactions with the pyrrole protons, their protons (with the exception of the phenyl para protons) experience two different magnetic environments, depending whether they are oriented toward the inside (endo) or the outside (exo) of the assembly. At room temperature the rotation around the $C_{meso}-C_{ring}$ bond is relatively fast on the NMR time scale, and the corresponding signals are averaged. Below −20 °C the rotation is slow on the NMR time scale, and endo and exo protons have resolved resonances. The endo protons are more shielded by the cofacial porphyrin and therefore resonate more upfield than the corresponding exo

(33) Kim, H.-J.; Bampos, N.; Sanders, J. K. M. *J. Am. Chem. Soc.* **1999**, *121*, 8120−8121.
(34) (a) Endo, A.; Okamoto, Y.; Suzuki, K.; Shimamura, J.; Shimizu, K.; Satô, G. P. *Chem. Lett.* **1994**, 1317−1320. (b) Endo, A.; Tagami, U.; Wada, Y.; Saito, M.; Shimizu, K.; Satô, G. P. *Chem. Lett.* **1996**, 243−244.
(35) Marvoud, V.; Launay, J.-P. *Inorg. Chem.* **1993**, *32*, 1376−1382.
(36) (a) Anderson, H. L.; Hunter, C. A.; Meah, M. N.; Sanders, J. K. M *J. Am. Chem. Soc.* **1990**, *112*, 5780−5789. (b) Anderson, H. L.; Anderson, S.; Sanders, J. K. M. *J. Chem. Soc., Perkin Trans. 1* **1995**, 2231−2245 and references therein.
(37) (a) Anderson, H. L. *Inorg. Chem.* **1994**, *33*, 972−981. (b) Wilson, G. S.; Anderson, H. L. *Chem. Commun.* **1999**, 1539−1540. (c) Taylor, P. N.; Anderson, H. L. *J. Am. Chem. Soc.* **1999**, *121*, 11538−11545.
(38) Drain, C. M.; Nifiatis, F.; Vasenko, A.; Batteas, J. D. *Angew. Chem., Int. Ed.* **1998**, *37*, 2344−2347.

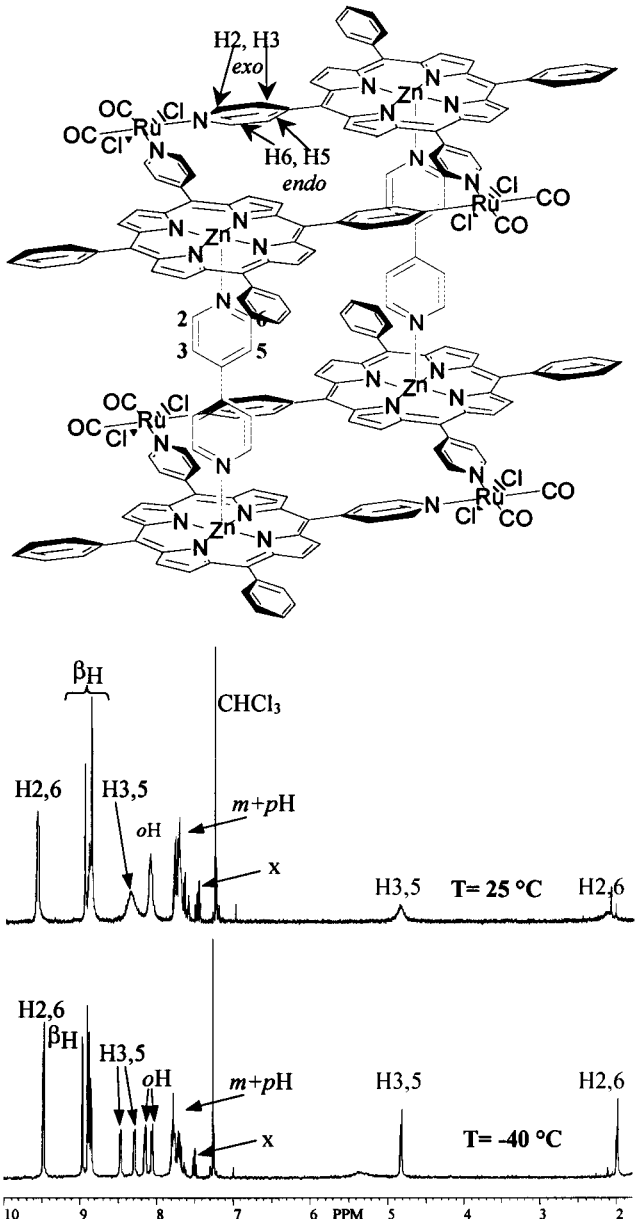

Figure 3. Schematic drawing of [(**5Zn**)$_2$(μ-4,4′-bipy)$_2$] (**7**) with labeling scheme and its ^{1}H NMR spectrum at 25 °C (top) and −40 °C (bottom); resonances of bridging 4,4′-bipy ligands are labeled H3,5 and H2,6 in the upfield region of the spectra; an impurity is marked with X.

protons. In agreement with this hypothesis, in the 2D EXSY spectrum of **7** at −20 °C each pair of resonances of endo and exo aromatic protons is connected by an exchange cross-peak.

Similarly to what was observed for **7**, ^{1}H NMR spectroscopy established that addition of a stoichiometric amount of 4′-*trans*-DPyP-npm or 4′-*trans*-DPyP to a $CDCl_3$ solution of **5Zn** leads to the quantitative formation of the corresponding sandwich adducts [(**5Zn**)$_2$(μ-4′-*trans*-DPyP-npm)$_2$] (**8**) or [(**5Zn**)$_2$(μ-4′-*trans*-DPyP)$_2$] (**9**), respectively. Compounds **8** and **9** are discrete supramolecular assemblies of molecular squares of metalloporphyrins axially connected through other porphyrins. During the titrations, no other derivatives are observed apart from the molecular sandwiches **8** or **9** and residual **5Zn**. The model trimeric compounds [(Zn·TPP)$_2$(μ-4′-*trans*-DPyP-npm)] (**10**) and [(Zn·TPP)$_2$(μ-4′-*trans*-DPyP)] (**11**) (TPP = 5,10,15,20-tetraphenylporphyrin) were also investigated for comparative purposes.

Assignments of the resonances of the two stacked molecular squares in **8** and **9** are very similar to those described above for compound **7**. As was the case for **7**, the resonances of the pyridyl and phenyl protons of the 4′-*cis*-DPyP units in **8** and **9**, slightly broad at room temperature, split into sharp signals below −20 °C. The dramatic upfield shift of the resonances of 4′-*trans*-DPyP-npm and 4′-*trans*-DPyP in **8** and **9**, respectively, indicate that they are axially bound to **5Zn** in a symmetric environment. The combined shielding effect decreases gradually as the proton distance from the zinc porphyrins increases. This is a common feature in the ^{1}H NMR spectra of axially ligated units in side-to-face arrays of porphyrins.[22] Thus, in the ^{1}H NMR spectrum of **8** (−20 °C), the multiplets at δ = 2.62 and δ = 6.06, correlated in the H−H COSY spectrum, were assigned respectively to H2,6 and H3,5 of coordinated 4′-*trans*-DPyP-npm. Very similar shifts for the pyridyl protons were observed in the NMR spectrum of **9**.

Interestingly, the internal −NH protons in **8** (δ = −3.62) and in **9** (δ = −4.10) resonate more than 0.2 ppm farther upfield compared to the same protons in the corresponding model compounds **10** (δ = −3.35) and **11** (δ = −3.89). The extra shielding that affects the bridging porphyrins in **8** and **9** compared to the reference compounds may be attributed to a mutual ring current effect of the two macrocycles assuming that, as an average, in solution they maintain the cofacial orientation found in the solid state (see below). Calculations based on the double-dipole model developed by Abraham et al. for TPP,[39] and on geometrical parameters derived from the molecular structure of **9** (see below), are in very good agreement with this hypothesis (calculated upfield shift of −NH resonance of ca. 0.25 ppm). These calculations show also that the shielding effects on each bridging porphyrin caused by the two laterally displaced chromophores belonging to the **5Zn** squares are negligible.

Overall, the above NMR features indicate that, at ambient temperature, the equilibrium between **5Zn** and **L** to yield [(**5Zn**)$_2$(μ-**L**)$_2$] has an intermediate to slow rate on the NMR time scale (relatively broad signals for **L**) and is totally shifted toward the 2:2 product (all or nothing process), suggesting that there must be considerable cooperativity between the addition of the first and the second bridging ligands. The sandwich compounds **7**−**9** can be directly compared with the simplest ladder structures investigated by Anderson and co-workers,[37] formed by two conjugated zinc porphyrin dimers connected by two bridging ligands (L = DABCO, 4,4′-bipy), and for which a formation constant of ca. 10^{18} M^{-2} was estimated in chloroform.[37c] However, in that case the zinc porphyrin dimers are flexible and undergo conformational rearrangements when forming the ladder; in our case the **5Zn** squares are rigid, thus entropy considerations (no global conformational changes required) should further favor the assembly of sandwich structures and formation constants higher than 10^{18} are to be expected (assuming that the electron donor/acceptor properties of **L** and **5Zn**, respectively, are comparable to those of the ligands and zinc porphyrins used by Anderson). In other words, the chelate effect of a rigid dimer such as **5Zn**, after binding the first bidentate ligand, is anticipated to be larger than that of a flexible dimer. Accordingly, the NMR spectra of $CDCl_3$

(39) Abraham, J. R.; Bedford, G. R.; McNeillie, D.; Wright, B. *Org. Magn. Reson.* **1980**, *14*, 418−424.

solutions of both **7** and **9**, diluted to the limit of detection (ca. 3×10^{-5} M), showed the resonances of the intact sandwich structure exclusively. For comparison, we obtained binding constants of about 10^6 M^{-2} for trimers **10** and **11** by NMR titration in $CDCl_3$, in good agreement with those found in the literature for similar systems.[36,37]

By using 0.1 mm path length quartz cuvettes, we could monitor the variations in the visible absorption spectrum during the formation of **7** from **5Zn** and 4,4′-bipy at the concentration used for NMR purposes (ca. 10^{-4} M); in the experiment, titration of 4,4′-bipy into a $CDCl_3$ solution of **5Zn** was monitored by ^{1}H NMR spectroscopy, and the solution was sampled by visible spectroscopy after each addition of the ligand. Unlike the systems investigated by Anderson and co-workers,[37] for which the remarkable conformational changes experienced by the flexible porphyrin strands upon ladder formation induced substantial modifications in the absorption spectra, in our case the spectrum of each sandwich assembly is essentially the sum of those of the constituents. When, according to NMR spectra, formation of **7** was completed, a bathochromic shift of ca. 7 nm was observed for the Soret band; this spectral change is typical for axial coordination of N ligands to zinc porphyrins.[40] Similar shifts were observed in the case of **8** and **9**, even though the final spectra are somehow more complicated because the absorption bands of the axial porphyrins overlap partially with those of the cofacial molecular squares. The photophysical investigation of **8** and **9** is currently in progress.

Finally, in all cases, gradual addition of excess bridging ligand to solutions of [(**5Zn**)$_2$(μ-**L**)$_2$] induces a progressive broadening of the NMR signals of **L** which eventually become undetectable, even at the lowest temperature in $CDCl_3$. This observation is in good agreement with what already found by Anderson and co-workers upon addition of excess bridging ligand to the molecular ladders of zinc porphyrin strands and can be explained with the establishment of a fast exchange between [(**5Zn**)$_2$(μ-**L**)$_2$], the open species [(**5Zn**)(**L**)$_2$] which bears monocoordinated **L**, and uncoordinated **L** (Scheme 2).[37]

X-ray Structure of [(5Zn)$_2$(μ-4′-*trans*-DPyP)$_2$] (9). Single crystals of **9** suitable for X-ray investigation were obtained by layering *n*-hexane on top of a $CDCl_3$ solution of the compound. The structural determination of compound **9** indicates that the molecular sandwich architecture observed in solution, containing two **5Zn** macrocycles axially connected face-to-face by two 4′-*trans*-DPyP ligands, is maintained also in the solid state (Figure 4). The pairs of **5Zn** units and 4′-*trans*-DPyP connecting ligands, referred by a center of symmetry, are slightly bowed outward and inward, respectively, as evidenced by the angle between the porphyrin least-squares planes inside the **5Zn** macrocycle (17.4(2)°) and by the angle Zn1−(4′-*trans*-DPyP core)−Zn2′ (167°). Thus, the Zn1···Zn2′ distance of 19.463(7) Å is only an approximate indication of the span of the 4′-*trans*-DPyP ligand. The two bridging porphyrins are cofacial, at a distance of 11.448 Å; this finding is consistent with the NMR data that indicated a similar arrangement for the two porphyrins also in solution. Two molecules of *n*-hexane are incapsulated in the cavity defined by this boxlike architecture.

The Zn ions have a square pyramidal coordination geometry. An analysis of the bond lengths, although at low accuracy,

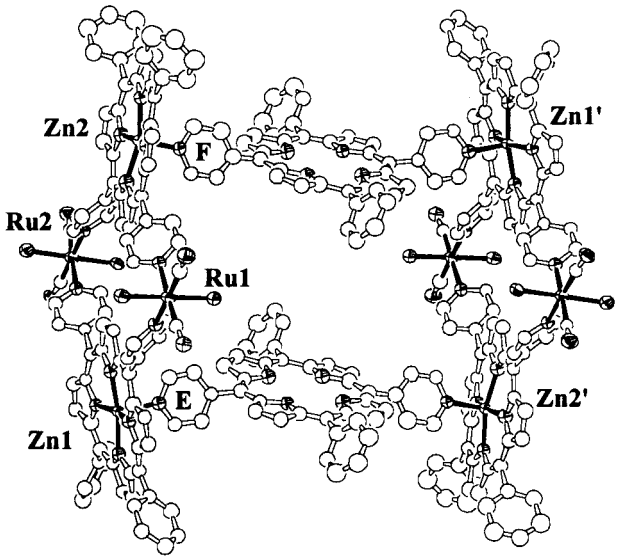

Figure 4. Perspective ORTEP drawing (40% probability for thermal ellipsoids) of the molecular sandwich [(**5Zn**)$_2$(μ-4′-*trans*-DPyP)$_2$] (**9**) with coordination bonds in solid. Selected distances (Å): Zn(1)···Ru(1) 9.940(4), Zn(1)···Ru(2) 9.837(4), Zn(2)···Ru(1) 9.917(4), Zn(2)···Ru(2) 9.957(4). Diagonals: Zn(1)···Zn(2) 13.532(4), Ru(1)···Ru(2) 14.454(5). 4′-*trans*-DPyP linkage: Zn(1)···Zn(2′) 19.463(7). The distance between the 4′-*trans*-DPyP porphyrin cores is 11.448 Å. Two molecules of *n*-hexane (not shown) are located inside the cavity.

reveals that two Zn−N(porphyrin) bond distances trans to one another (range 2.01(2)−2.06(2) Å) are slightly shorter than the others (2.10(2)−2.14(2) Å). The apical Zn−N(py) bond lengths are longer (2.15(2), 2.20(2) Å), with the metals displaced by 0.22 and 0.31 Å, respectively, toward the N donor. The 4-N(py) rings (E and F in Figure 4) bound to the Zn ions at apical positions are approximately perpendicular to the ZnN4 basal plane (86.2(4) and 86.7(5)°). The coordination bond distances about Ru ions do not present unusual values and are comparable with those found in other six-coordinate Ru(II) complexes.[28, 41]

X-ray Structure of [(5Zn)(μ-4,4′-bipy)]$_\infty$ (7). Crystals of **7** were obtained with the same technique as for **9**. However, the X-ray analysis of compound **7** showed that the solid-state architecture of this compound is different from that found in solution and consists of an infinite wire of **5Zn** squares bridged by 4,4′-bipy ligands which are axially coordinated alternatively on the two opposite sides of each square, [(**5Zn**)(μ-4,4′-bipy)]$_\infty$ (Figure 5). Two crystallographically different **5Zn** macrocycles, A and B, alternate along the chain, forming a stairlike infinite structure featuring the (ABA)·(ABA) motif, with inversion centers located between two consecutive ABA triplets and in the center of units B. The least-squares plane calculated for unit B is slanted by about 37° with respect to the adjacent macrocycle A, while two consecutive units A are parallel at a distance of ca. 25 Å. The stairlike wires are packed in a herringbone pattern.

The Zn(1)···Zn(3) and Zn(2)···Zn(2′) distances, which represent the 4,4′-bipy linkage spans, are similar (11.360(4) and 11.369(4) Å, respectively). The best-fit planes through the porphyrins (maximum deviations of atoms ±0.08 and ±0.12 Å) in the **5Zn** unit A make a dihedral angle of 13.90(8)°, indicating a slight tilt between them. This value is considerably smaller with respect to that observed in the cation [*trans*,*cis*,-

(40) Hunter, C. A.; Meah, M. N.; Sanders, J. K. M. *J. Am. Chem. Soc.* **1990**, *112*, 5773−5780.

(41) Alessio, E.; Milani, B.; Bolle, M.; Mestroni, G.; Faleschini, P.; Todone, F.; Geremia, S.; Calligaris M. *Inorg. Chem.* **1995**, *34*, 4772−4734.

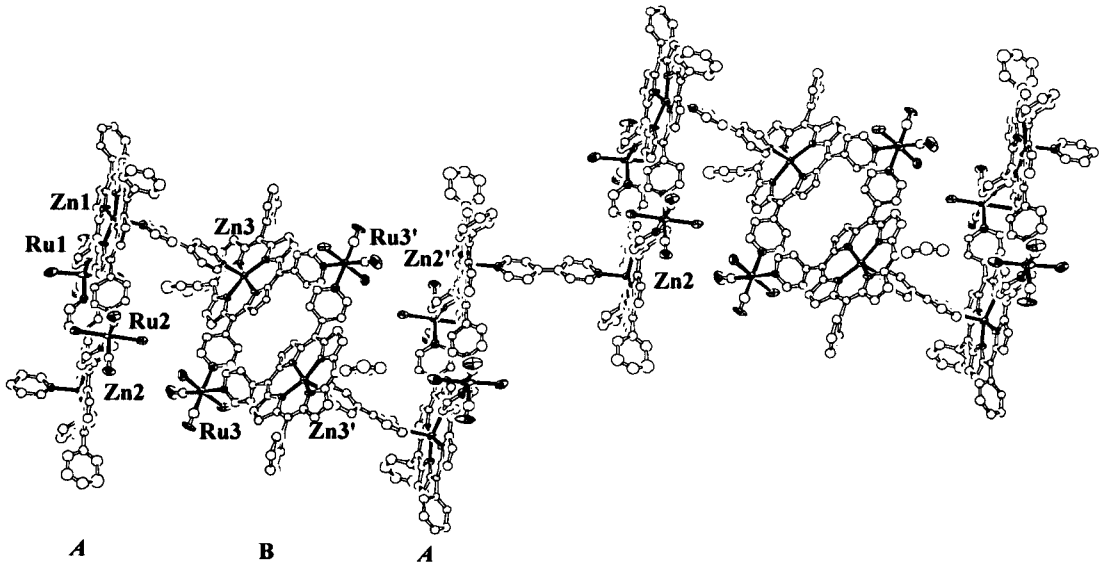

Figure 5. ORTEP drawing (40% probability for thermal ellipsoids) of the one-dimensional polymeric structure of compound [(**5Zn**)(μ-4,4′-bipy)]$_\infty$ (**7**) viewed down the crystallographic *c* axis. Side metal−metal distances (Å): Zn(1)···Ru(1) 9.868(3), Zn(1)···Ru(2) 9.917(3), Zn(2)···Ru(1) 9.904(3), Zn(2)···Ru(2) 9.918(3), Zn(3)···Ru(3) 9.895(3), Zn(3)···Ru(3′) 9.903(3). 4,4′-bipy linkages: Zn(1)···Zn(3) 11.360(4), Zn(2)···Zn(2′) 11.369(4). Diagonals: Zn(1)···Zn(2) 13.753 (4), Ru(1)···Ru(2) 14.249(4), Zn(3)···Zn(3′) 13.696(5), Ru(3)···Ru(3′) 14.296(4).

cis-$RuCl_2(CO)_2$(4′-*cis*-DPyP)$_2$Pd(dppp)]$^{2+}$ (41.7(1)°).[28] On the other hand, in the unit B the two porphyrins are almost coplanar, although with significant displacements of atoms from their mean plane (±0.38 Å).

The Zn and Ru ions display square pyramidal and octahedral coordination spheres, respectively, both with severe distortions from the ideality. The Zn−N bond distances in the basal plane, in the range 2.051(11)−2.097(10) Å, are slightly shorter, as expected, with respect to those involving the bipy nitrogen at the apex of the pyramid (from 2.123(11) to 2.179(10) Å), the Zn ions being displaced by about 0.3 Å toward the N atom. A view down the Ru···Ru vector for the macrocycles A and B evidences a twist of about 20° between the bipy rings g and h and a noticeable bending of pyridyl rings with respect to the basal ZnN4 planes, with dihedral angles of 72.1(4), 88.1(5), and 80.8(3)° for Zn1, Zn2, and Zn3, respectively (Figure 6). This unsymmetrical coordination of the bipy rings accounts for the canting of the units A and B described above.

The different structures found for **7** in solution (discrete, [(**5Zn**)$_2$(μ-4,4′-bipy)$_2$]) and in the solid state (polymeric, [(**5Zn**)-(μ-4,4′-bipy)]$_\infty$) require the presence of an equilibrium between the two forms: very likely solubility reasons drive the equilibrium toward the polymeric arrangement upon crystallization. In solution, the discrete sandwich structure [(**5Zn**)$_2$(μ-4,4′-bipy)$_2$] of **7** is very stable in the concentration range investigated, and there is no spectroscopic evidence of detectable amounts of polymeric or oligomeric material. Crystals of **7** redissolved in $CDCl_3$ yield the typical ^{1}H NMR spectrum of the sandwich structure.

The polymeric chain structure found for **7** in the solid state is an unprecedented example of a molecular wire made of porphyrin metallacycles bridged by organic ligands. Fujita and co-workers described recently the X-ray structure of an infinite stairlike polymer made of [Pt(en)(4,4′-bipy)]$_4^{8+}$ molecular squares linked at two adjacent corners by [$PtBr_2$(en)$_2$]$^{2+}$ complexes through Pt(II)···Br—Pt(IV) bridges.[42] To our knowledge, Fujita's work is the only previous example of structural characterization of a system in which molecular squares were purposefully used as building blocks for the construction of higher dimensional structures.[43] Other examples of solid-state arrays that might resemble the above systems, in that they define square-shaped repetitive patterns (e.g., extended polymeric

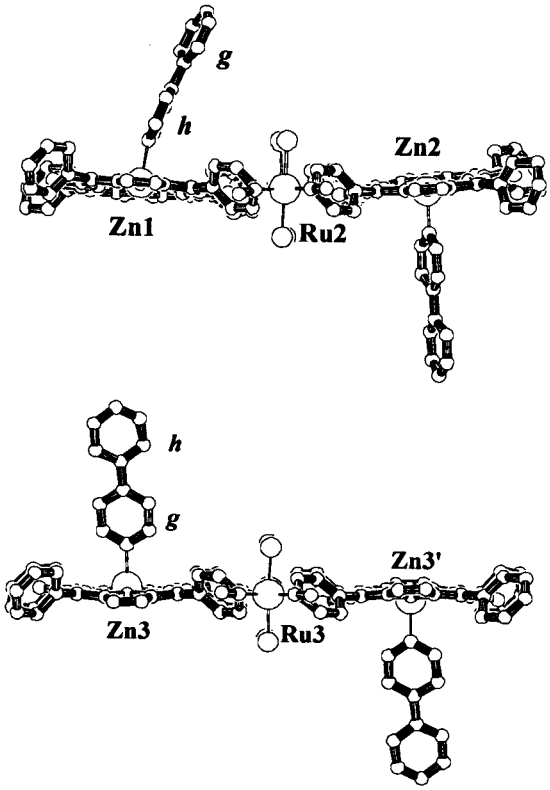

Figure 6. View of the two crystallographic **5Zn** macrocycles in compound [(**5Zn**)(μ-4,4′-bipy)]$_\infty$ (**7**), along the Ru(2)···Ru(1) (top) and Ru(3)···Ru(3′) (bottom) directions, showing the distortions of the coordinated bipy ligands.

(42) Aoyagi, M.; Biradha, K.; Fujita, M. *Bull. Chem. Soc. Jpn.* **1999**, *72*, 2603−2606.
(43) The assembling principle used by Fujita is actually different from ours, in that the structural metal corners of the squares are involved in the bridges.

networks of ladders[44] or square grids[45,46]), belong more properly to the field of crystal engineering. They were prepared by a completely different synthetic approach that does not involve preformed molecular squares but simply requires the mixing of a bridging ligand (either a porphyrin or not) and an appropriate metal ion capable of providing the required number of 90° connections.

Conclusions and Future Perspectives

In this work we described some new neutral 2+2 metallacycles made of porphyrins and octahedral ruthenium coordination compounds of formula [*trans*,*cis*,*cis*-$RuCl_2$(dmso-S)$_2$(4′-*cis*-DPyP)]$_2$ (**4**), [*trans*,*cis*,*cis*-$RuCl_2(CO)_2$(4′-*cis*-DPyP)]$_2$ (**5**), and [*trans*,*cis*,*cis*-$RuCl_2$(dmso-S)(CO)(4′-*cis*-DPyP)]$_2$ (**6**); the latter exists as an equimolar mixture of geometrical isomers **6a** and **6b**. Compared to most previous examples of molecular squares of porphyrins, which used square planar charged Pt(II) and Pd(II) complexes as structural units,[17,19−21] the metallacyclic species **4**−**6** are neutral, thus providing greater solubility in organic solvents. Moreover, the two additional coordinated "spectator" ligands in the octahedral complexes at each corner, beside being, in principle, useful extra spectroscopic handles for the characterization, might prove advantageous for a better fine-tuning of the properties of the metal and for further functionalization of the assemblies as well.

We also showed how these discrete units, after metalation of the porphyrins, are suitable building blocks for the construction of more elaborate supramolecular arrays by axial coordination of bridging ligands. This is made possible by the inertness of the Ru−pyridyl bond, which provides kinetic stability to the molecular squares **4**−**6**. In particular, introduction of zinc centers inside the porphyrin cores of the molecolar square **5**, followed by treatment with 1 equiv of trans ditopic N-donor ligands **L** (**L** = 4,4′-bipy, 5,15-bis(4′-pyridyl)-2,8,12,18-tetra-*n*-propyl-3,7,13,17-tetramethylporphyrin (4′-*trans*-DPyP-npm), or 5,15-bis(4′-pyridyl)-10,20-diphenylporphyrin (4′-*trans*-DPyP)), leads selectively to the quantitative assembling of sandwich-like supramolecular adducts of stacked metallacycles of porphyrins of formula [(**5Zn**)$_2$(μ-**L**)$_2$]. Single-crystal X-ray investigations showed that, depending on the nature of the bridging ligand, in the solid state these sandwich structures can either be maintained or originate polymeric chains, [(**5Zn**)(μ-**L**)]$_\infty$.

When **L** = 4′-*trans*-DPyP, both solution- and solid-state data indicate that [(**5Zn**)$_2$(μ-4′-*trans*-DPyP)$_2$] (**9**) can be regarded as a molecular box featuring two coplanar bridging porphyrins at a distance of about 11.4 Å. Even though cofacial bisporphyrins connected to one another by flexible or rigid organic bridges are well known,[36,47] systems in which the two porphyrins are not covalently linked are rather uncommon. A very recent example of a porphyrin-based capsule constructed through Pd(II)−pyridine bonds was reported by the group of Shinkai.[48] We are currently investigating the capability of **9** to behave as a host for the inclusion of guest molecules of appropriate shape and size through $\pi-\pi$ interactions with the cofacial porphyrins.

Scheme 3. Expected Formation of Nanotubes with Six-Coordinate Metal Ions (M)

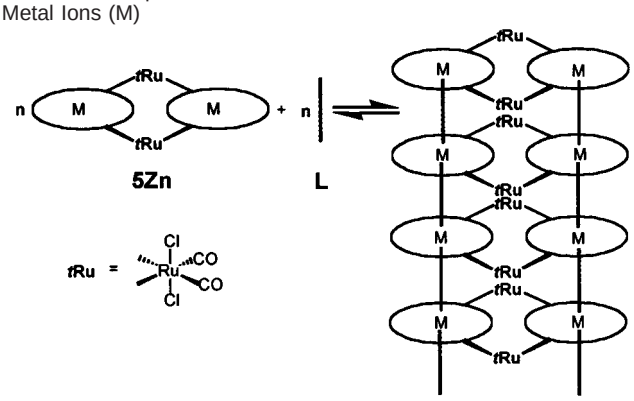

When **L** = 4,4′-bipy, the corresponding adduct **7** has the anticipated sandwich-like discrete architecture [(**5Zn**)$_2$(μ-4,4′-bipy)$_2$] in solution, but it assumes a stairlike polymeric wire structure [(**5Zn**)(μ-4,4′-bipy)]$_\infty$ in the solid state. The polymer [(**5Zn**)(μ-4,4′-bipy)]$_\infty$ is made of **5Zn** squares bridged by 4,4′-bipy ligands which are axially coordinated alternatively on the two opposite sides of each square.

Compared to the previous work by Anderson and co-workers, in which axial coordination was used to introduce rigidity into flexible zinc porphyrin oligomers and increase conjugation,[37] our work has a different aim, i.e., the construction of discrete 3D supramolecular assemblies of porphyrins delimiting cavities of well-defined shape and size; for this purpose we introduced the use of zinc porphyrin metallacycles as rigid 2D building blocks. Apart from the general aim, our approach presents some distinctive features: (1) the structural metal centers of our building blocks might introduce useful photophysical and redox properties into the supramolecular assemblies and be exploited for their further functionalization; (2) the rigid frame of the zinc porphyrin metallacycles involves a lower entropic tribute in the assembly process, therefore leading to higher thermodynamic stability of the adducts; moreover, the rigid frame of the molecular squares ensures that the bridging ligands are arranged at a fixed distance and with a well-defined mutual orientation; (3) the shape of the 3D porphyrin assemblies obtained by this approach depends on the nature of the metal ions inserted in the molecular squares. In principle, while five-coordinate metal ions such as Zn lead to the formation of discrete sandwich-like molecular boxes, as shown in this work, six-coordinate metal ions (e.g., Mg, Co, Sn) should allow the stacking of multiple layers of metallacycles, thus leading to polymeric nanotubes that define a cavity of the inner size of the squares (Scheme 3). Work in this direction with larger (4+4) molecular squares is currently in progress in our laboratory.

Experimental Section

General Methods. Hydrated $RuCl_3$ was a loan from Johnson Matthey. *trans*-$RuCl_2$(dmso-S)$_4$ (**1**), *trans*-$RuCl_2$(dmso-O)$_2(CO)_2$ (**2**), and *trans*-$RuCl_2$(dmso)$_3$(CO) (**3**) were prepared according to literature procedures.[41,49] 4′-*cis*-DPyP and 4′-*trans*-DPyP were prepared and separated as described by Fleischer and Shacter.[16] 4′-*trans*-DPyP-npm

(44) Losier, P.; Zaworotko, M. J. *Angew. Chem., Int. Ed. Engl.* **1996**, *35*, 2779−2782.
(45) Subramanian, S.; Zaworotko, M. J. *Angew. Chem., Int. Ed. Engl.* **1995**, *34*, 2127−2129.
(46) Sharma, C. V. K.; Broker, G. A.; Huddleston, J. G.; Baldwin, J. W.; Metzger, R. M.; Rogers, R. D. *J. Am. Chem. Soc.* **1999**, *121*, 1137−1144.
(47) For a recent review, see: Chang, C. J.; Deng, Y.; Heyduk, A. F.; Chang, C. K.; Nocera, D. G. *Inorg. Chem.* **2000**, *39*, 959−966.
(48) Ikeda, A.; Ayabe, M.; Shinkai, S.; Sakamoto, S.; Yamaguchi, K. *Org. Lett.* **2000**, *2*, 3070−3710.
(49) Alessio, E.; Mestroni, G.; Nardin, G.; Attia, W. M.; Calligaris, M.; Sava, G.; Zorzet, S. *Inorg. Chem.* **1988**, *27*, 4099−4106.

was prepared and purified as reported.[50] All reagents were analytical grade. Thin-layer chromatography was performed on silica plates (Merck) using as eluent a 95/5 chloroform/ethanol mixture. Column chromatography was performed on 40−63 μm mesh silica gel (BDH). UV−vis spectra were obtained on a Jasco V-550 spectrometer in quartz cells (path length 0.1, 1, or 10 mm), using CH_2Cl_2 freshly distilled over dry $CaCl_2$ as solvent. ^{1}H NMR and ^{13}C NMR spectra were recorded at 400 and 100.5 MHz, respectively, on a JEOL Eclipse 400 FT instrument. All spectra were run at room temperature in $CDCl_3$ (Aldrich), unless differently stated. Proton peak positions were referenced to the peak of residual nondeuterated chloroform set at 7.26 ppm. Carbon peak positions were referenced to the central peak of chloroform set at 77.0 ppm. Assignments were made with the aid of 2D correlation spectroscopy (H−H COSY) and of 2D exchange spectroscopy (EXSY) experiments as detailed in the text; a mixing time of 500 ms was used for EXSY experiments. Solution ($CHCl_3$) infrared spectra were recorded in 0.1 mm cells with NaCl windows on a Perkin-Elmer 983G spectrometer. FAB-MS measurements were done on a JEOL JMS-SX102/SX102A/E at Emory University (Atlanta, GA).

X-ray Crystallography. Data collections for compounds **7** and **9** were performed at the X-ray diffraction beamline of Elettra Synchrotron (Trieste, Italy) on a 30 cm MAR2000 image plate with a monochromatic wavelength of 1.000 Å using the rotating crystal method. The temperature was kept at 100 K by using a nitrogen stream cryo-cooler. The data reduction and cell refinement were carried out by using the program MOSFLM.[51] Both structures were solved by standard Patterson[52] and Fourier methods and refined by full-matrix least-squares on F^2[53] using the WinGX System, Ver. 1.63.[54] In compound **7**, the pyridyl ligands at Ru1, as well as the bipy rings at Zn2, were found conformationally disordered over two positions (occupancies factors of 0.48/0.52, 0.48/0.52, and 0.38/0.62). A difference Fourier map revealed the presence of 3.5 molecules of $CHCl_3$ and 0.5 molecule of *n*-hexane per asymmetric unit in **7**, and of an *n*-hexane molecule in **9**. Additional solvent molecules, included in the formulas of both compounds, were used for density calculation, by taking into account the analysis of the accessible voids in the unit cell obtained with the Platon package.[55] Final cycles of refinement with the contribution of hydrogen atoms placed at geometrically calculated positions (except those of disordered pyridyl rings in compound **7**) converged to the *R* factors reported in Table 1.

[*trans*,*cis*,*cis*-RuCl$_2$(dmso-S)$_2$(4′-*cis*-DPyP)]$_2$ (4). A mixture of 26 mg of 4′-*cis*-DPyP (0.04 mmol) and 18.7 mg of **1** (0.04 mmol) dissolved in 5 mL of $CHCl_3$ was allowed to react for 5 h at room temperature. Thin-layer chromatography of the crude product showed it to contain **4** (R_f = 0.72) together with other minor species. Pure **4** was obtained as the first band from a column (4 × 10 cm) eluted with chloroform. Yield: 18.5 mg (49%). ^{1}H NMR spectrum ($CDCl_3$): δ = 10.05 (m, 8H, H2,6), 9.05 (s, 4H, βH), 8.98 (d, 4H, βH), 8.90 (m, 8H, βH), 8.41 (m, 8H, H3,5), 8.24 (m, 8H, *o*H), 7.82 (m, 12H, *m*+*p*H), 3.65 (s, 24H, dmso-S), −2.75 (s, 4H, NH). UV−vis spectrum (λ_{max} (nm), $\epsilon \times 10^{-4}$ (cm^{-1} M^{-1})) in CH_2Cl_2: 425 (50.0), 518 (5.0), 554 (3.5), 591 (3.0), 646 (2.5). FAB mass spectrum: *m*/*z* 1892.1 (M^+), calcd for $C_{92}H_{80}N_{12}Cl_4O_4S_4Ru_2$ 1890.

[*trans*,*cis*,*cis*-RuCl$_2$(CO)$_2$(4′-*cis*-DPyP)]$_2$ (5). A procedure similar to that described for **4** was followed; reaction time, 16 h. Pure **5** (R_f = 0.73) was obtained as the first band from a column (4 × 10 cm) eluted with chloroform. Yield from 30 mg of 4′-*cis*-DPyP and a stoichiometric amount of **2**: 18 mg (46%). ^{1}H NMR spectrum ($CDCl_3$): δ = 9.83 (m, 8H, H2,6), 9.08 (m, 4H, βH), 9.04 (m, 8H, βH), 8.91 (s, 4H, βH), 8.58 (m, 8H, H3,5), 8.26 (m, 8H, *o*H), 7.85 (m,12H, *m*+*p*H), −2.72 (s, 4H, NH). Selected ^{13}C NMR resonances ($CDCl_3$): δ = 194.9 (CO). UV−vis spectrum (λ_{max} (nm), $\epsilon \times 10^{-4}$ (cm^{-1} M^{-1})) in CH_2Cl_2: 426 (50.0), 519 (4.5), 555 (3.0), 591 (2.5), 647 (2). Selected IR bands ($CHCl_3$): 2073 and 2013 cm^{-1} (ν(C═O)). FAB mass spectrum: *m*/*z* 1691.2 (M^+), calcd for $C_{88}H_{56}N_{12}Cl_4O_4Ru_2$ 1690.

[*trans*,*cis*,*cis*-RuCl$_2$(dmso-S)(CO)(4′-*cis*-DPyP)]$_2$ (6). A procedure similar to that described for **4** was followed; reaction time, 16 h. Pure **6** (R_f = 0.73) was obtained as the first band from a column (4 × 10 cm) eluted with a 99/1 chloroform/ethanol mixture. Yield from 30 mg of 4′-*cis*-DPyP and a stoichiometric amount of **3**: 20 mg (51%). ^{1}H NMR spectrum ($CDCl_3$): δ = 10.08 (m, 4H, H2,6 trans to dmso-S), 9.65 (m, 4H, H2,6 trans to CO), 9.11 (m, 4H, βH), 9.06 (s, 4H, βH), 8.90 (s, 8H, βH), 8.58 (m, 4H, H3,5 trans to dmso-S), 8.47 (m,4H, H3,5 trans to CO), 8.26 (m, 8H, *o*H), 7.83 (m,12H, *m*+*p*H), 3.71 (s, 12H, dmso-S), −2.72 (s, 4H, NH)). Selected ^{13}C NMR resonances ($CDCl_3$): δ = 200.6 (CO). UV−vis spectrum (λ_{max} (nm), $\epsilon \times 10^{-4}$ (cm^{-1} M^{-1})) in CH_2Cl_2: 425 (45.0), 519 (2.5), 555 (1.2), 593 (0.8), 648 (0.5). Selected IR bands ($CHCl_3$): 1990 cm^{-1} (ν(C═O)). FAB mass spectrum: *m*/*z* 1790.5 (M^+), calcd for $C_{90}H_{68}N_{12}Cl_4O_4S_2Ru_2$ 1790.

[*trans*,*cis*,*cis*-RuCl$_2$(CO)$_2$(Zn·4′-*cis*-DPyP)]$_2$ (5Zn). A 25 mg amount of **5** (0.012 mmol) dissolved in 5 mL of $CHCl_3$ was treated with an 8-fold molar excess of $Zn(CH_3COO)_2$ (18.4 mg) dissolved in the minimum amount of MeOH. Samples of the reaction mixture were periodically withdrawn, diluted in CH_2Cl_2, and sampled by visible spectroscopy. The spectrum indicated that the zinc insertion was complete (after ca. 16 h) when the four Q-bands of **5** collapsed to two bands (552 and 590 nm); the Soret band shifted from 426 to 428 nm, accompanied by a decrease of intensity ($\epsilon = 32 \times 10^4$ cm^{-1} M^{-1} for **5Zn** vs $\epsilon = 50 \times 10^4$ cm^{-1} M^{-1} for **5**). These spectral changes are similar to those found upon metalation of free porphyrins.[16] The product was precipitated by addition of *n*-hexane, removed by filtration, washed throughly with cold methanol and diethyl ether, and vacuum-dried. Yield: 16.5 mg (75%). R_f = 0.45. ^{1}H NMR spectrum ($CDCl_3$): δ = 9.82 (m, 8H, H2,6), 9.18 (m, 4H, βH), 9.15 (m, 8H, βH), 9.04 (s, 4H, βH), 8.58 (m, 8H, H3,5), 8.26 (m, 8H, *o*H), 7.84 (m, 12H, *m*+*p*H). UV−vis spectrum (λ_{max} (nm), $\epsilon \times 10^{-4}$ (cm^{-1} M^{-1})) in CH_2Cl_2: 428 (32), 552 (2), 590 (0.5).

[(5Zn)$_2$(μ-4,4′-bipy)$_2$] (7), [(5Zn)$_2$(μ-4′-*trans*-DPyP-npm)$_2$] (8), and [(5Zn)$_2$(μ-4′-*trans*-DPyP)$_2$] (9). ^{1}H NMR titrations were performed adding small amounts of each ligand (4,4′-bipy, 4′-*trans*-DPyP-npm,

Table 1. Crystallographic Data for Compounds **7** and **9**

compound	**7**·0.5*n*-hexane·5.5($CHCl_3$)	**9**·3*n*-hexane·1.5(CH_2Cl_2)
formula	$C_{155.5}H_{102.5}Cl_{22.5}N_{21}O_6Ru_3Zn_3$	$C_{149.5}H_{125}Cl_7N_{18}O_4Ru_2Zn_2$
fw	3653.30	2815.00
cryst system	triclinic	triclinic
space group	$P\bar{1}$	$P\bar{1}$
a, Å	17.272(4)	11.923(4)
b, Å	23.772(5)	21.890(4)
c, Å	25.077(5)	27.183(6)
α, deg	87.54(2)	69.06(2)
β, deg	84.13(2)	84.87(2)
γ, deg	76.96(2)	89.00(2)
V, Å^3	9976(4)	6599(3)
Z, D_{calcd}, g cm^{-3}	2, 1.216	2, 1.417
$2\theta_{max}$, deg	53.62	47.16
no. of unique reflcs	14124	6465
no. of obsd data [$I > 2\sigma(I)$]	8929	3859
no. of parameters	990	716
μ, mm^{-1}	2.271	1.896
GOF (F^2)	1.037	1.002
R1(F_o), wR2 (F_o^2)[a]	0.0865, 0.2465	0.0972, 0.2555

[a] $R1 = \sum||F_o| - |F_c||/\sum|F_o|$, $wR2 = [\sum w(F_o^2 - F_c^2)^2/\sum w(F_o^2)^2]^{1/2}$.

(50) (a) Senge, M. O.; Medforth, C. J.; Forsyth, T., P.; Lee, D. A.; Olmstead, M. M.; Jentzen, W.; Pandey, R. K.; Shelmut, J. A.; Smith K. M. *Inorg. Chem.* **1997**, *36*, 1149−1163. (b) Sessler, J. L.; Hugdahl, J.; Johnson M. R. *J. Org. Chem.* **1986**, *51*, 2838−2840.
(51) Leslie, A. G. W. *Jnt CCP4/ESF-EACMB Newslett. Protein Crytallogr.* **1992**, *26*.
(52) Sheldrick, G. M. *Acta Crystallogr., Sect. A* **1990**, *A46*, 467−473.
(53) Sheldrick, G. M. SHELXL-97, Program for crystal structure refinement; University of Göttingen, Germany, 1997.
(54) Farrugia, L. J. *J. Appl. Crystallogr.* **1999**, *32*, 837−838.
(55) Spek, A. L. *Acta Crystallogr., Sect. A* **1990**, *A46*, C-34.

and 4′-*trans*-DPyP) to a ca. 10^{-3} M $CDCl_3$ solution of **5Zn** in a 5 mm NMR tube. When, according to NMR spectra, formation of compounds **7**, **8**, and **9** was complete, the products were isolated upon removal of the solvent. Purple crystals of **7** and **9** suitable for X-ray diffraction were obtained by slow diffusion of *n*-hexane into a $CDCl_3$ solution of **7** and **9**.

7. ^{1}H NMR spectrum ($CDCl_3$, −40 °C): δ = 9.48 (m, 16H, H2,6, **5Zn**), 8.97 (s, 8H, βH), 8.88 (m, 24H, βH), 8.47 (d, 8H, H3,5, **5Zn**, exo), 8.29 (d, 8H, H3,5, **5Zn**, endo), 8.14 (d, 8H, *o*H, exo), 8.05 (d, 8H, *o*H, endo), 7.77 (m, 16H, *m*+*p*H, exo), 7.67 (m, 8H, *m*H, endo), 4.81 (d, 4H, H3,5, 4,4′-bipy), 1.99 (d, 4H, H2,6, 4,4′-bipy). UV−vis spectrum (λ_{max} (nm)) in CH_2Cl_2: 431.0 (Soret), 565.0, and 607.0 (Q-bands).

8. ^{1}H NMR spectrum ($CDCl_3$, −20 °C): δ = 9.71 (d, 8H, H2,6, **5Zn**, exo), 9.64 (s, 4H, mesoH), 9.56 (d, 8H, H2,6, **5Zn**, endo), 9.15 (m, 32H, βH), 8.65 (d, 8H, H3,5, **5Zn**, exo), 8.60 (d, 8H, H3,5, **5Zn**, endo), 8.30 (m, 16H, *o*H), 7.83 (m, 16H, *m*H, exo, +*p*H), 7.76 (m, 8H, *m*H, endo), 6.06 (d, 8H, H3,5, 4′-*trans*-DPyP-npm), 3.34 (m, 16H, $-CH_2CH_2CH_3$), 2.62 (d, 8H, H2,6, 4′-*trans*-DPyP-npm), 1.78 (m, 16H, $-CH_2CH_2CH_3$), 0.85 (m, 48H, $-CH_2CH_2CH_3 + -CH_3$), −3.62 (s, 4H, NH). UV−vis spectrum (λ_{max} (nm)) in CH_2Cl_2: 430.0 (Soret), 510.0, 559.0, and 604.5 (Q-bands).

9. ^{1}H NMR spectrum ($CDCl_3$, −55 °C): δ = 9.60 (d, 8H, H2,6, **5Zn**, exo), 9.46 (d, 8H, H2,6, **5Zn**, endo), 9.18 (m, 24H, βH, **5Zn**), 9.03 (s, 8H, βH, **5Zn**), 8.66 (m, 16H, H3,5, **5Zn**), 8.34 (m, 16H, *o*H, **5Zn,** endo + βH, 4′-*trans*-DPyP), 8.28 (m, 8H, *o*H, **5Zn**, exo), 7.83 (m, 24H, *m*H, **5Zn**, exo + *p*H, **5Zn** + βH, 4′-*trans*-DPyP), 7.78 (m, 8H, *m*H, **5Zn,** endo + βH, 4′-*trans*-DPyP), 7.57 (d, 8H, *o*H, 4′-*trans*-DPyP), 7.31 (m, *m*+*p*H, 4′-*trans*-DPyP), 6.25 (d, 8H, H3,5, 4′-*trans*-DPyP), 2.56 (d, 8H, H2,6, 4′-*trans*-DPyP), −4,10 (s, 4H, NH). UV−vis spectrum (λ_{max} (nm)) in CH_2Cl_2: 420.0, and 430.5 (Soret bands), 516.0, and 560.0 (Q-bands).

[(Zn·TPP)$_2$(μ-4′-*trans*-DPyP-npm)] (10), [(Zn·TPP)$_2$(μ-4′-*trans*-DPyP)] (11). These compounds were obtained by NMR titration. To a $CDCl_3$ solution (ca. 5 mM) of 4′-*trans*-DPyP-npm or 4′-*trans*-DPyP, respectively, were added weighed amounts of Zn·TPP, and the ^{1}H NMR spectra were recorded. Zn·TPP was added until the chemical shifts of the adducts did not change; in both cases, a ca. 6-fold excess of Zn·TPP was required. At this stage the temperature was lowered to the value required for comparison with the spectra of compounds **8** and **9**. The apparent K_f values at room temperature (ca. 10^6) were obtained by nonlinear regression analyses of the chemical shifts data (for H2,6, H3,5, and −NH) versus concentration of Zn·TPP. The fit of the data was made using the software package Scientist.[56]

10. ^{1}H NMR spectrum ($CDCl_3$, −20 °C): δ = 9.82 (s, mesoH), 8.97 (s, βH*), 9.26 (m, *o*H*), 9.77 (m, *m*+*p*H*), 6.20 (d, H3,5), 3.58 (m, $-CH_2CH_2CH_3$), 2.82 (d, H2,6), 1.87 (m, $-CH_2CH_2CH_3$), 0.98 (m, $-CH_2CH_2CH_3 + -CH_3$), −3.35 (s, NH).

11. ^{1}H NMR spectrum ($CDCl_3$, −55 °C), selected resonances: δ = 8.99 (s, βH, Zn·TPP*), 8.50 (d, βH, 4′-*trans*-DPyP), 8.27 (m, *o*H−Zn·TPP*), 7.79 (m, *m*+*p*H−Zn·TPP*), 7.40 (d, βH, 4′-*trans*-DPyP), 6.32 (d, H3,5), 2.79 (d, H2,6), −3.89 (s, NH).

(Note: for **10** and **11** ^{1}H NMR data, asterisks indicate that the resonances relative to coordinated Zn·TPP overlap with those of excess Zn·TPP; therefore, relative integration with signals of 4′-*trans*-DPyP-npm in **10** and 4′-*trans*-DPyP in **11** was not possible.)

Acknowledgment. We thank the Italian MURST for financial support, Johnson Matthey for a loan of hydrated $RuCl_3$, and Prof. Luigi G. Marzilli (Emory University, Atlanta, GA) for recording the FAB-MS spectra. This work was performed in the frame of EU Program COST, Action D11 "Supramolecular Chemistry", project no. 0004/98. Staff assistance at the crystallographic beam line of the synchrotron facility of ELETTRA (Trieste, Italy) is gratefully acknowledged.

Supporting Information Available: Tables of crystal data, structure solution and refinement, atomic coordinates, bond length and angles, and anisotropic thermal parameters for **7** and **9**; ^{1}H NMR spectra for **5** and **5Zn**; ^{1}H NMR, H−H COSY, and FAB-MS spectra for **6**; low-*T* H−H COSY and EXSY spectra for **7**; low-*T* ^{1}H NMR spectrum for **8**; visible spectra of **5Zn** and **7**; side view of molecular structure of **9**; crystal packing for **7**; NMR titration leading to **11** (PDF); X-ray crystallographic data (CIF). This material is available free of charge via the Internet at http://pubs.acs.org.

JA016162S

(56) Scientist 2.01; MicroMath Scientific Software, Salt Lake City, UT, 1995.